Steel and Composite Structures, *Vol. 22, No. 4 (2016) 821-835*
DOI: http://dx.doi.org/10.12989/scs.2016.22.4.821

Experimental behavior of circular flyash-concrete-filled steel tubular stub columns

Yang Zhang [1,2], Guang-Yuan Fu [1], Chen-Jiang Yu [1], Bing Chen [3], She-Xu Zhao [1] and Si-Ping Li [*1]

[1] *Department of Engineering Mechanics, Shanghai Jiao Tong University, Shanghai 200240, P.R. China*
[2] *School of Civil Engineering, Nanyang Institute of Technology, Nanyang 473004, P.R. China*
[3] *Department of Civil Engineering, Shanghai Jiao Tong University, Shanghai 200240, P.R. China*

(*Received September 19, 2015, Revised October 18, 2016, Accepted October 28, 2016*)

Abstract. The paper presents an experimental study of the structural behavior of circular flyash-concrete-filled steel tubular stub columns under axial compressive loads. In this study, 90% and 100% by weight of the cement in the concrete core was replaced with flyash. Twenty-seven specimens were tested to study the influence of flyash content, wall thickness of the steel tube, and curing age on the ultimate capacity and confinement effect. The experimental results were compared with the design values calculated using AISC-LRFD (1999), ACI (1999), AIJ (1997) and Eurocode 4 (1994). From the experimental study, it was determined that the confinement effect of circular steel tubes filled with high content flyash concrete was better than that of specimens filled with ordinary Portland cement concrete. The 5.88-mm-thick steel tube filled with 100% flyash concrete was equivalent in strength to a steel tube filled with C30 concrete at 28 days.

Keywords: flyash-concrete-filled steel tubes; stub columns; ultimate load-carrying capacity; confinement effect

1. Introduction

Concrete-filled steel tubular (CFST) columns have been increasingly used in modern structures, such as high-rise buildings, bridges, barriers, and subway platforms, in recent decades. CFST columns have excellent mechanical properties, including a high load capacity, high stiffness, high ductility, low strength degradation, and high capacity for energy absorption (Abdalla *et al*. 2013, Kvedaras *et al*. 2015, Jiang *et al*. 2010, Xiao *et al*. 2012, Chung *et al*. 2013, Chen *et al*. 2011, Abed *et al*. 2013, Evirgen *et al*. 2014), which is due to the interaction between the steel tube and its concrete core caused by the discrepancy between the Poisson's ratios of steel and concrete. The external steel tube prevents the lateral expansion of the concrete core, and the concrete core prevents the local inward buckling of the steel tube.

Flyash is a type of industrial waste that is primarily produced by coal-fired power plants. Currently, the world's annual production of flyash is enormous, but its rate of utilization is still very low. Mixing flyash into concrete not only helps to reduce costs and protect the environment

*Corresponding author, Professor, E-mail: lisp_sjtu@sina.com

http://www.techno-press.org/?journal=scs&subpage=6 ISSN: 1229-9367 (Print), 1598-6233 (Online)

but also improves the quality of concrete in terms of better durability, lower heat generation, and higher compactness (Dinakar 2012, Siddique 2011, Bilodeau and Malhotra 2000, Kayali and Ahmed 2013, Dinakar *et al*. 2013). However, replacing the cement with flyash significantly influences the concrete's strength. Research into CFST columns has been conducted around the world for many years, and many findings have been obtained. Most of the existing studies focus on CFST columns containing no flyash or a small amount of flyash, and there has no research into CFST columns using pure flyash as a cementitious material until now.

Gupta *et al*. (2007) experimentally investigated the behavior of circular steel tubular columns filled with self-compacting flyash concrete with flyash contents of 15%, 20% and 25%. The results revealed that, for a given deformation, the load carrying capacity decreased as flyash content increased until the latter reached 20%; it increased again when flyash content reached 25%. Li *et al*. (2006) experimentally studied the effects of flyash contents of 10%, 20% and 40% and curing ages of 28 days, 56 days, 120 days and 210 days on the strength of CFST stub columns. The results showed that lower flyash contents improved the compressive strength and the bond strength and that a higher flyash content required more time to have similar beneficial effects.

Because flyash is a type of high-yield waste that is suitable for mixing into concrete to make it more durable and economical, it is meaningful to investigate the mechanical performance of flyash-concrete-filled steel tubular (CFFST) stub columns. The objective of this investigation is threefold: first, to report a series of experimental results for CFFST stub columns subjected to axial compressive loads; second, to investigate the effects of wall thickness of the steel tube, flyash content, and curing age on the behavior of axially loaded circular CFFST stub columns; and third, to compare the experimental results with the design values calculated using the existing codes.

2. Details of the experiments

2.1 Materials

The cement used was ordinary Portland cement. Class II flyash (conforming to Chinese standard GB/T 1596-2005) from the Shanghai Wujing Power Plant was selected for the study. The results of a chemical analysis of the cementitious materials used are presented in Table 1. The coarse aggregate was gravel with the particle size varying from 5 mm to 31.5 mm. The fine aggregate was river sand with the fineness modulus of 2.8.

Table 1 Chemical composition of the cementitious materials (%)

	Cement	Flyash
Silicon dioxide (SiO_2)	21.6	50.66
Aluminum oxide (Al_2O_3)	4.13	35.58
Ferric oxide (Fe_2O_3)	4.57	5.11
Calcium oxide (CaO)	64.44	1.94
Magnesium oxide (MgO)	1.06	1.09
Sodium oxide (Na_2O)	0.11	0.40
Potassium oxide (K_2O)	0.56	0.34
Sulfur trioxide (SO_3)	1.74	0.37
Loss on ignition	0.76	4.07

Table 2 Concrete mixes (kg/m^3)

Series	Flyash content	W/B	Cement	Flyash	Sand	Gravel	Water	Activator
F000	0	0.44	450.0	—	553	1176	198	—
F090	90%	0.44	45.0	405.0	553	1176	198	—
F100	100%	0.44	—	427.5	553	1176	198	22.5

Table 3 Physical properties of the steel tubes

Series	Wall thickness (mm)	Modulus of elasticity (GPa)	Yield strength (MPa)	Tensile strength (MPa)	Elongation (%)
H243	2.43	206	289.9	373.8	20.0
H424	4.24	206	277.5	442.7	14.7
H588	5.88	206	272.2	472.5	18.7

The control concrete (F000) was mixed in accordance with Chinese standard JGJ 55-2011, and then, the flyash concrete was mixed by replacing some of the cement with the same weight of flyash. The activator comprised of 60% cement and 40% sodium silicate was used only in the concrete containing 100% flyash (F100). The mixes are shown in Table 2.

Each of the steel tubes used had uniform dimensions with an outer diameter of 115 mm and length of 400 mm. Three types of steel plate with wall thicknesses of 2.43 mm, 4.24 mm and 5.88 mm were studied. A 6-mm-thick endplate was welded to the bottom of each steel tube. All of the steel tubes were made from mild steel (Q235). To determine the physical properties of steel, strip coupons were cut from randomly-selected steel tubes and tested under tension in accordance with Chinese standard GB/T 228-2002. The physical properties of the steel tubes are listed in Table 3.

2.2 Casting, curing and testing

Three 100 mm cube specimens were cast for studying the compressive strength of each type of concrete. Cement, flyash, sand, and activator were poured into a 100 liter planetary mixer and mixed for approximately 1 minute, and then, the remaining components were poured into the mixture and mixed until a uniform and flowing mixture was obtained. The fresh concrete was poured into molds and compacted by hand. Demolding was performed after 24 hours, 7 days and 15 days for the F000, F090 and F100 concrete samples, respectively. Except for the F100 concrete specimens, which were placed in air and sprayed with water twice a day, all of the specimens were cured in water. The compressive strength of the concrete specimens is presented in Table 4.

Fresh concrete was also poured into steel tubes and compacted using a vibrator. The top surface of each specimen was sealed with a polyethylene sheet for curing. Details of the CFFST specimens are shown in Table 5. A total of 27 CFFST specimens, including 9 specimens filled with control concrete and 18 specimens filled with flyash concrete, were tested on a 2000 kN compression testing machine. All of the specimens were loaded continuously till failure at a rate of 0.5 kN/s. The test arrangement is shown in Fig. 1. A linear voltage displacement transducer (LVDT) was used to monitor the axial deformation. Four groups of strain gauges were evenly distributed around the middle cross section of each specimen for measuring the longitudinal and transverse strains of the steel tube. The specimen was seated directly on the rigid steel bed of the testing

machine, and a 28-mm-thick bearing plate was placed on top of the specimen. Prior to the actual test, a 10 kN pre-load was applied to ensure a close contact between the platens of the testing machine and the ends of the specimen.

Table 4 Compressive strength of the concrete mixtures (MPa)

Series	Compressive strength		
	28 d	90 d	210 d
F000	37.8	—	—
F090	6.0	6.3	6.2
F100	1.2	—	—

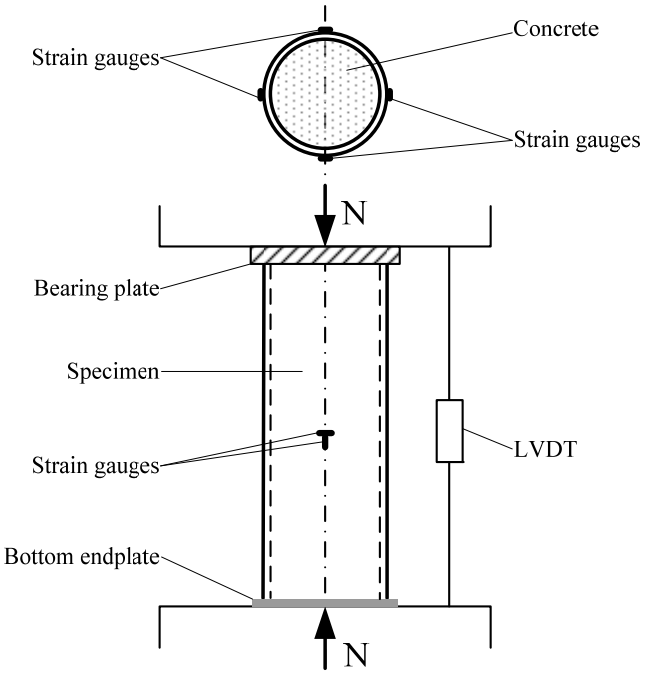

Fig. 1 A schematic view of the test setup

Table 5 Details of the CFFST specimens

Series*	Length (mm)	Outer diameter (mm)	Wall thickness (mm)	Flyash content (%)	Curing age (d)	N_{exp} (kN)	Confinement (%)
CH243F000A028	400	115	2.43	0	28	656.4	23.1
CH424F000A028	400	115	4.24	0	28	1078.2	59.7
CH588F000A028	400	115	5.88	0	28	1385.8	73.6
CH243F090A028	400	115	2.43	90	28	403.3	37.0
CH424A090A028	400	115	4.24	90	28	764.2	69.2

Table 5 Continued

Series*	Length (mm)	Outer diameter (mm)	Wall thickness (mm)	Flyash content (%)	Curing age (d)	N_{exp} (kN)	Confinement (%)
CH588F090A028	400	115	5.88	90	28	1144.0	94.5
CH243F100A028	400	115	2.43	100	28	358.1	38.6
CH424F100A028	400	115	4.24	100	28	654.5	56.8
CH588F100A028	400	115	5.88	100	28	1047.2	88.3
CH243F090A090	400	115	2.43	90	90	453.3	53.1
CH424F090A090	400	115	4.24	90	90	856.4	88.9
CH588F090A090	400	115	5.88	90	90	1156.5	96.1
CH243F090A210	400	115	2.43	90	210	445.2	50.2
CH424F090A210	400	115	4.24	90	210	878.9	94.0
CH588F090A210	400	115	5.88	90	210	1186.5	101.2

*C—circular steel tube; HXXX—wall thickness of the steel tube;
FYYY—weight percent of cement replaced with flyash; AZZZ—curing age

Fig. 2 CFFST specimens after the experiments

Fig. 3 A typical failure mode

3. Experimental results and discussion

3.1 The typical failure mode of CFFST stub columns

Fig. 2 shows a photograph of the CFFST specimens used in the experiments. The typical failure mode is shown in Fig. 3. All of the specimens collapsed by local buckling, and specimens that failed in the typical mode swelled similar to drums and formed folds in their middles. The thin-walled CFFST specimens formed more folds than the thick-walled specimens, as shown in Fig. 2.

3.2 The load-deformation curve of the CFFST stub columns

Fig. 4 shows the experimental load-deformation (N-ε) curves of the CFFST specimens. The axial load (N) is plotted against the longitudinal strain (ε) and transverse strain (ε_T) on the same graph. The influence of flyash content and curing age on the N-ε curve is closely related to the steel tube's wall thickness (as shown in Fig. 4). The N-ε curves of the thick-walled specimens with different flyash contents are more similar to each other, as shown in Fig. 4(c). The lateral expansion of the specimens filled with F090 and F100 concrete primarily occurred early and

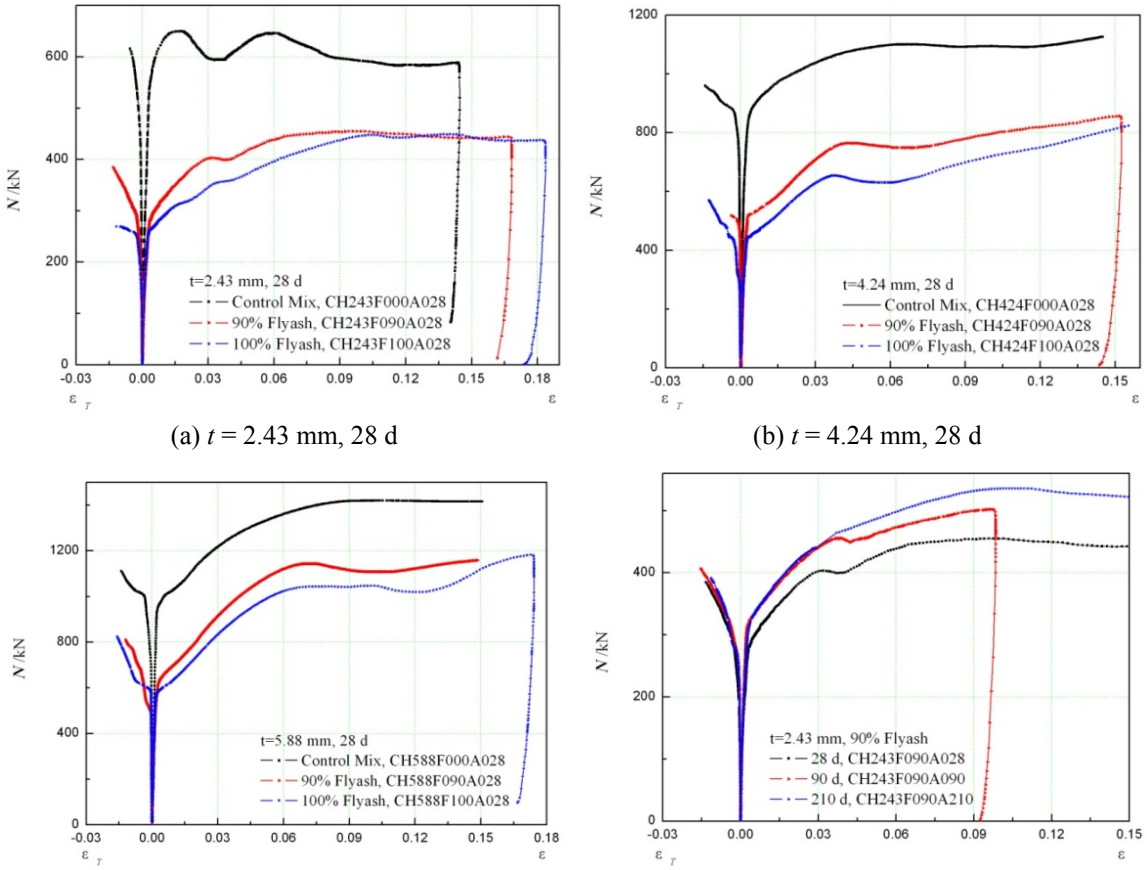

(a) t = 2.43 mm, 28 d (b) t = 4.24 mm, 28 d

(c) t = 5.88 mm, 28 d (d) t = 2.43 mm, 90% flyash

Fig. 4 Load-deformation curves of CFFST stub columns

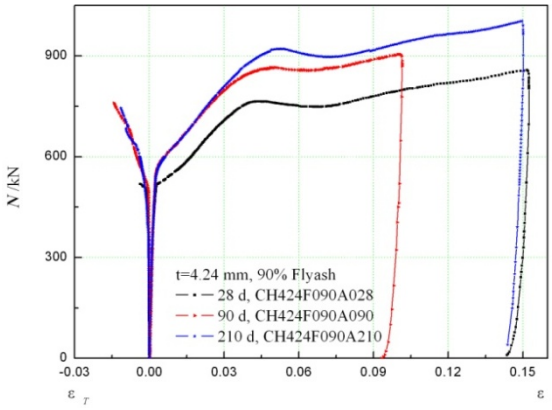

(e) t = 4.24 mm, 90% flyash

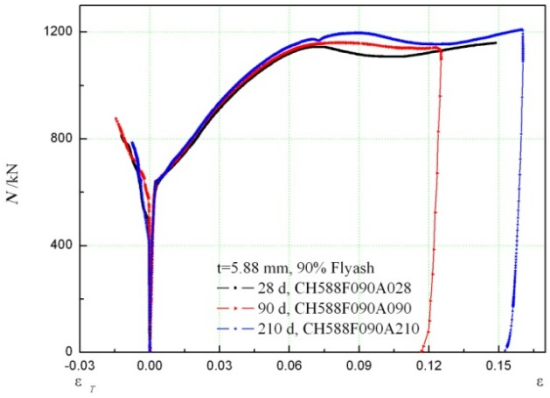

(f) t = 5.88 mm, 90% flyash

Fig. 4 Continued

developed more rapidly than that of the specimens filled with control concrete as the load grew gradually. The N-ε curves of specimens CH588F090A028, CH588F090A090 and CH588F090A210 were nearly coincident, as shown in Fig. 4(f), indicating that the difference between the N-ε curves of the CFFST specimens at different curing ages decreased with the steel tube's wall thickness.

The typical N-ε curve of a CFFST stub column can be divided into four stages, which are shown in Fig. 5:

Stage I (o-a): The elastic stage: There is a proportional increase of the deformation with the load. In this stage, the deformation of a CFFST stub column was too small to be observed.

Stage II (a-b): The yield stage: There is a nonlinear increase of the deformation with the load. In this stage, the steel tube began to yield and the sound of the concrete core

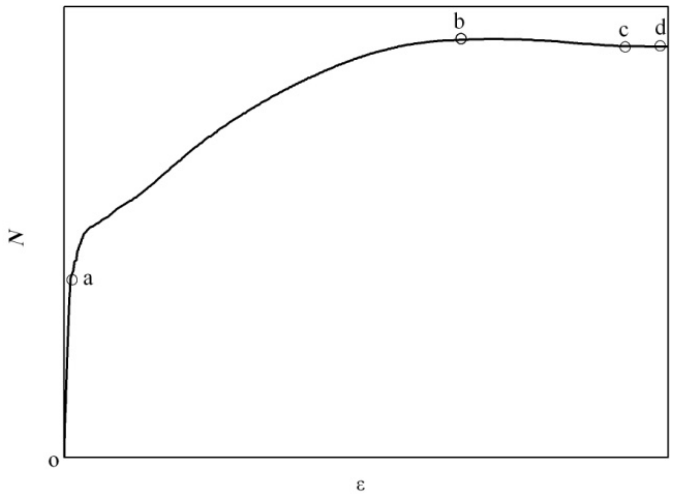

Fig. 5 A typical load-deformation curve of a CFFST stub column

cracking could be heard occasionally. As the load reached point b (the maximum load), local buckling and lateral expansion of the steel tube could be easily observed with the naked eye.

Stage III (b-c): The descending stage of the load-deformation curve: In this stage, the load began to decrease slightly and the deformation increased faster. Obvious folds formed on the surface of the external steel tube.

Stage IV (c-d): The strengthening stage of the load-deformation curve: In this stage, the residual strength of the CFFST stub columns was generally constant, and the deformation continued to increase rapidly.

3.3 The ultimate capacity of the CFFST stub columns

The experimental ultimate loads of the CFFST specimens are listed in Table 5. Fig. 6 shows the influences of flyash content, wall thickness and curing age on the ultimate load. The ultimate load decreases as flyash content increases because an ultra-high content of flyash reduces the strength of the concrete core significantly (as seen in Fig. 6(a)). Compared with the 28-day specimens filled with control concrete, the ultimate load of the 28-day specimens filled with F090 concrete decreases by 38.6%, 29.1% and 17.4%, respectively, and the ultimate load of the 28-day specimens filled with F100 concrete decreases by 45.4%, 39.3% and 24.4%, respectively.

The ultimate load is positively correlated with wall thickness because steel tubes with thick walls can not only withstand greater loads but also provide stronger circumferential confinement to concrete core (seen from Fig. 6(b)). For 28-day specimens filled with control concrete, F090 concrete and F100 concrete, as the wall thickness varies from 2.43 mm to 4.24 mm, the ultimate load increases by 64.3%, 89.5%, and 82.8%, respectively, and the ultimate load increases by 111.1%, 183.7%, and 192.4%, respectively for a wall thickness of 5.88 mm.

The influence of curing age on the ultimate load is less than those of flyash content and wall thickness. The ultimate load increases slowly and slightly with time from 28 days onward (seen from Fig. 6(c)). Due to the low pozzolanic activity of flyash, a pozzolanic reaction slowly occurs between the vitreous silicates in flyash, which include silicon dioxide and aluminum oxide, and the alkaline substances in cement. Concrete with a very high flyash content does not include enough cement to maintain a pozzolanic reaction, As a result, the ultimate capacity develops relatively rapidly in the first 90 days, and then, it gradually slows down. Compared with the 28-day specimens filled with F090 concrete, the ultimate load of the 90-day specimens increases by 12.4%, 12.1%, and 1.1%, respectively.

3.4 Analysis of the confinement effect

The ultimate capacity depends primarily on the external steel tube's confinement of the concrete core. As long as sufficient confinement is provided, the bearing capacity of specimens filled with ultra-low-strength concrete is satisfactory because when the concrete core is in a triaxial stress state, its strength and ductility are enhanced. For example, the 28-day compressive strength of the F100 concrete is only 3.1% of that of the control concrete, and for 2.43 mm, 4.24 mm, and 5.88 mm wall thickness, the ultimate capacities of the specimens filled with F100 concrete are 54.6%, 60.7% and 75.6%, respectively, of the ultimate capacity of specimens filled with the control concrete.

The confinement effect is expressed by the ratio of the difference between the experimental ultimate load and its theoretical value to the theoretical value. The theoretical ultimate load is

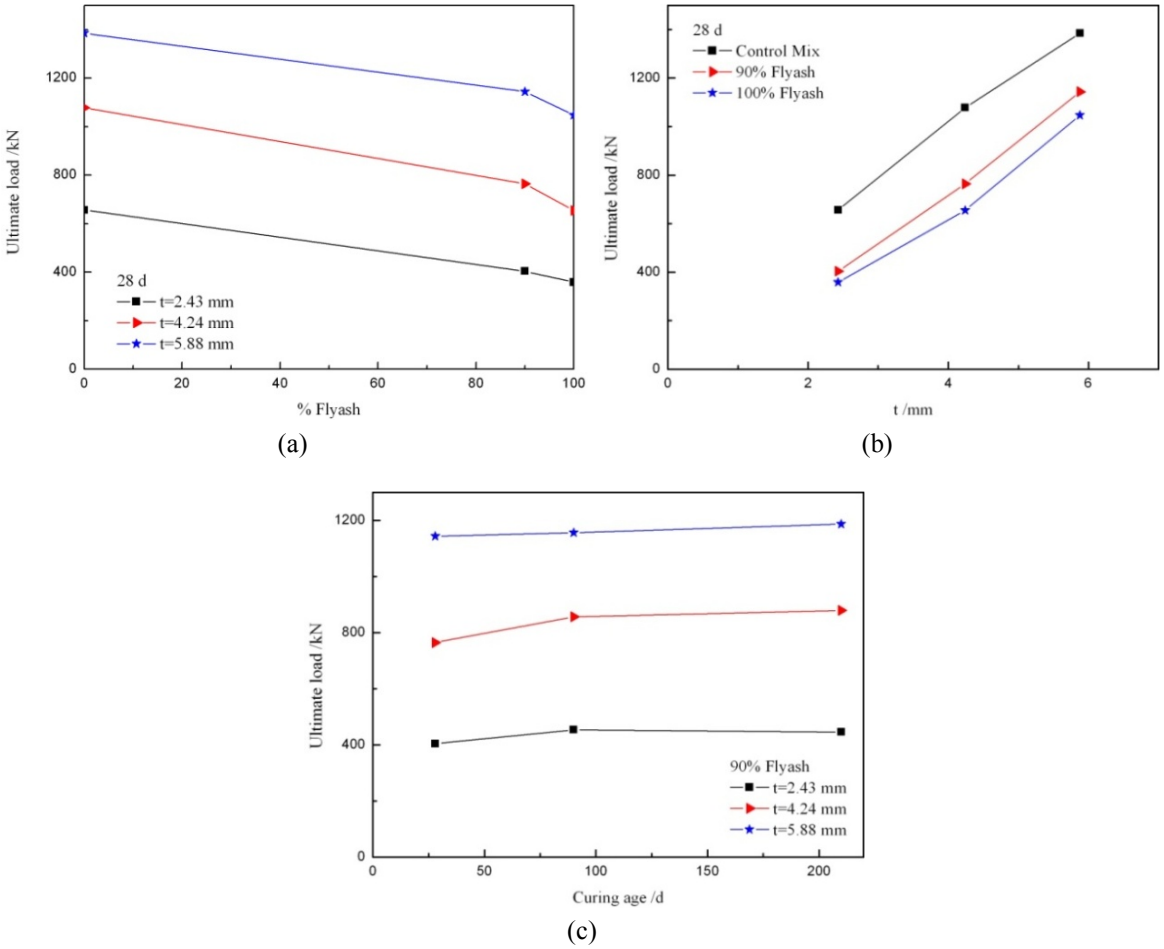

Fig. 6 Influence of (a) flyash content; (b) wall thickness; and (c) curing age on the ultimate capacity of CFFST stub columns

calculated by summing the individual peak values of the steel tube and the concrete core without considering the enhancement of the concrete's strength that is due to the confinement effect. The confinement percentages are listed in Table 5. The confinement percentage of specimen CH588F090A210 is the largest of 101.2%. Fig. 7 shows the influence of flyash content, wall thickness and curing age on the confinement percentage.

For the wall thickness of 4.24 mm and 5.88 mm, the confinement percentage increases with flyash contents of up to 90% and decreases for higher flyash contents (seen from Fig. 7(a)). The flyash mixed into the concrete reduces the concrete's porosity due to a microfiller effect; therefore, flyash concrete is more compact than ordinary Portland cement concrete. A concrete core with a flyash content of 90% has not only a certain strength but is also very compact, which leads to a high confinement percentage.

The confinement percentage is positively correlated with wall thickness and curing age. The 28-day confinement percentage of specimens filled with control, F090 and F100 concrete increases by 158.7%, 87.1%, and 47.2%, respectively, when the wall thickness increases from 2.43 mm to

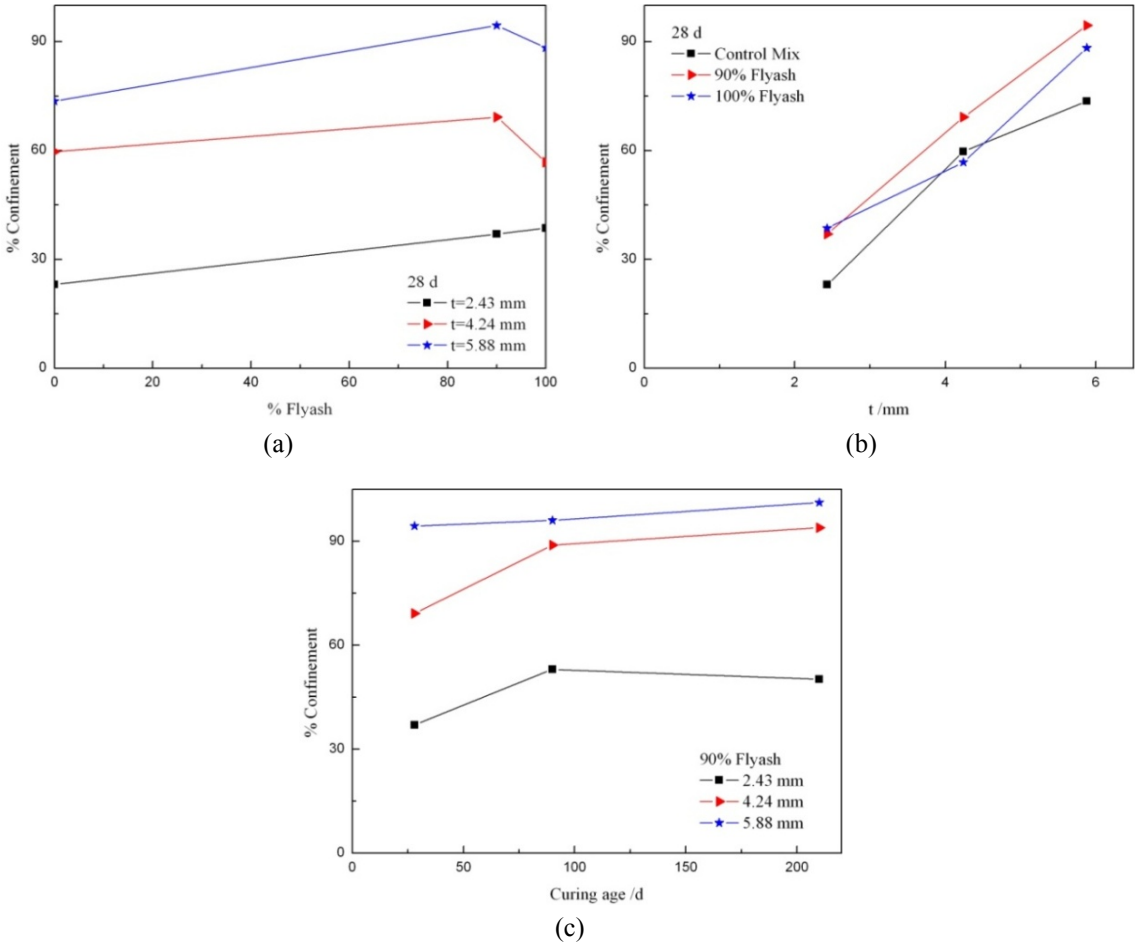

Fig. 7 Influence of (a) the flyash content; (b) the wall thickness; and (c) the curing age on the confinement percentage of CFFST stub columns

4.24 mm, and the 28-day confinement percentage increases by 218.9%, 155.4%, and 128.8%, respectively, for a wall thickness of 5.88 mm. Compared with the 28-day specimens filled with F090 concrete, the confinement percentage of the 90-day specimens increases by 43.5%, 28.5%, and 1.7%, respectively.

Fig. 8 shows the relationship between the axial load (N) and the strain ratio (v) of the CFFST specimens. The strain ratio is defined as the absolute value of the lateral strain divided by the axial strain, and the values are the averages of the axial and the lateral strain measured using strain gauges. An increase in the strain ratio indicates an increase in confinement effect of the concrete core produced by the external steel tube. The strain ratio of all of the specimens is approximately 0.3 during the elastic stage, and it begins to increase rapidly when the load reaches the critical load that indicates that the confinement effect of the steel tube is occurring. Compared with the specimens filled with control concrete, the critical load of the specimens filled with F090 and F100 concrete is lower, and the strain ratio develops more rapidly beyond the critical load, indicating that the confinement effect of specimens filled with high-content flyash concrete appears earlier

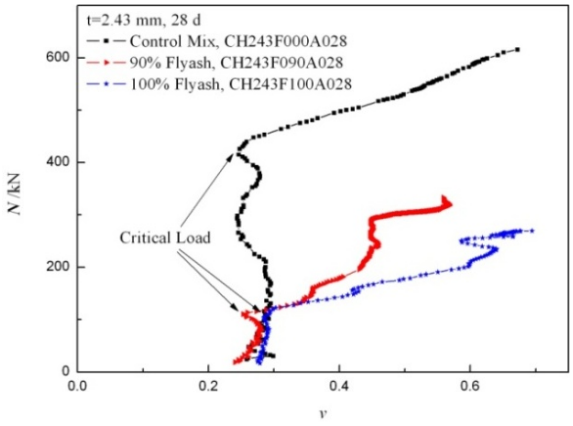

(a) t = 2.43 mm, 28 d

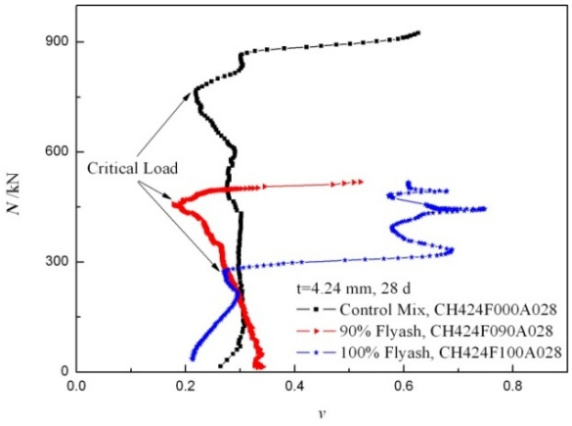

(b) t = 4.24 mm, 28 d

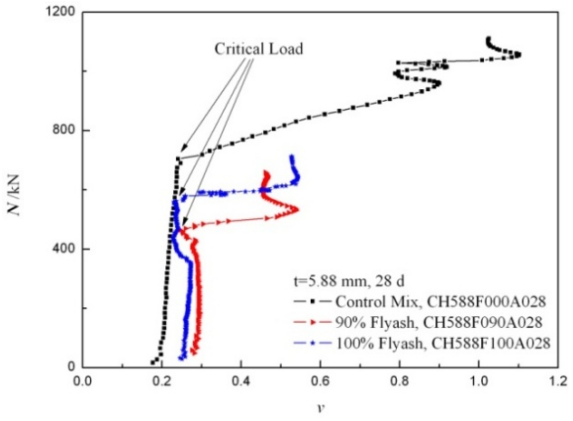

(c) t = 5.88 mm, 28 d

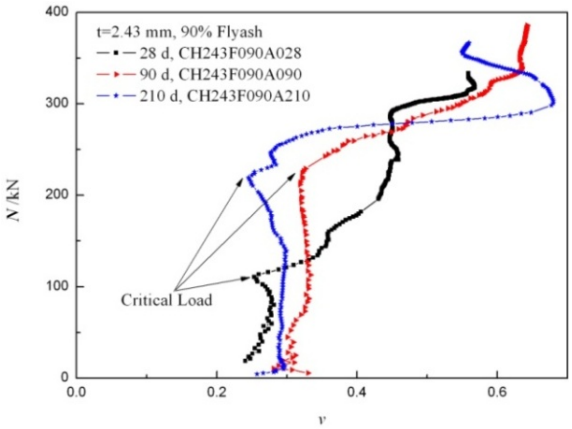

(d) t = 2.43 mm, 90% flyash

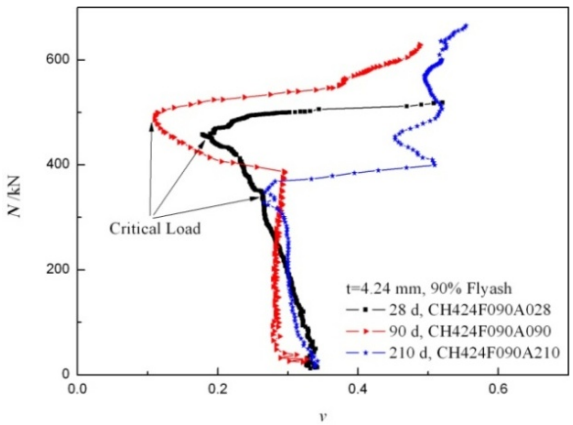

(e) t = 4.24 mm, 90% flyash

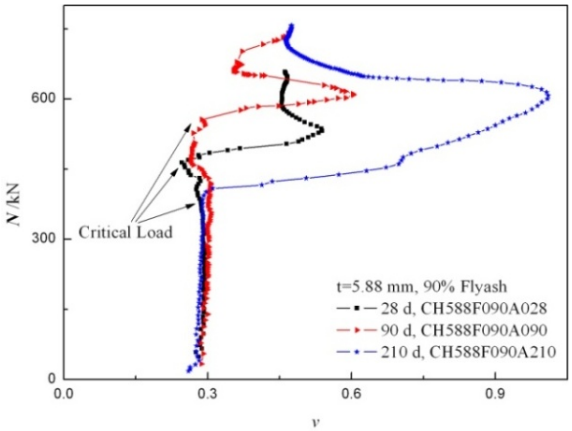

(f) t = 5.88 mm, 90% flyash

Fig. 8 Load-strain ratio curves of CFFST stub columns

(as shown in Figs. 8(a), 9(b)-(c)). The critical load of the 2.43-mm-thick specimens filled with F090 concrete at 90 days and 210 days is much greater than it is at 28 days, which indicates the time effect (as shown in Fig. 8(d)).

3.5 Comparison and evaluation of the results

A comparison of the experimental results with ultimate loads estimated using AISC-LRFD (1999), ACI (1999), AIJ (1997), and Eurocode 4 (1994) is presented in Table 6. AISC-LRFD, ACI, AIJ, and Eurocode 4 conservatively underestimate the ultimate load by 73.3%, 72.0%, 70.9%, and 22.9%, respectively. The mean and standard deviation of the Eurocode 4 results are 1.229 and 0.172, respectively. It can be concluded that AISC-LRFD, ACI and AIJ are excessively conservative in their predictions of the ultimate capacities of CFST stub columns and that Eurocode 4 provides more reasonable predictions, which is consistent with previous research (Han *et al*. 2005).

Fig. 9 shows a comparison of the experimental ultimate loads of specimens filled with F090 and F100 concrete with the ultimate load of a specimen filled with C10, C20 or C30 concrete predicted using Eurocode 4. For a wall thickness of 2.43 mm, the bearing capacity of specimens filled with F090 concrete is not equal to that of specimens filled with C10 concrete until 90 days. For a wall thickness of 4.24 mm, specimens filled with F090 concrete can be used as specimens filled with C20 concrete at 28 days, and at 90 days they are equivalent in strength to specimens filled with C30 concrete. For a wall thickness of 5.88 mm, specimens filled with F090 and F100 concrete are equal in strength to specimens filled with C30 concrete at 28 days.

Table 6 A comparison of the experimental results with those of AISC-LRFD, ACI, AIJ, and Eurocode 4

Specimen	N_{exp} (kN)	N_{LRFD} (kN)	N_{ACI} (kN)	N_{AIJ} (kN)	N_{EC4} (kN)	$\frac{N_{exp}}{N_{LRFD}}$	$\frac{N_{exp}}{N_{ACI}}$	$\frac{N_{exp}}{N_{AIJ}}$	$\frac{N_{exp}}{N_{EC4}}$
CH243F000A028	656.4	484.9	490.7	503.4	620.8	1.354	1.338	1.304	1.057
CH424F000A028	1078.2	629.3	635.2	647.1	829.5	1.713	1.697	1.666	1.300
CH588F000A028	1385.8	754.3	760.7	771.9	1001.9	1.837	1.822	1.795	1.383
CH243F090A028	403.3	285.6	287.6	289.6	410.7	1.412	1.402	1.393	0.982
CH424A090A028	764.2	442.4	445.3	447.2	634.9	1.727	1.716	1.709	1.204
CH588F090A028	1144.0	578.5	582.3	584.1	819.2	1.978	1.965	1.959	1.396
CH243F100A028	358.1	254.9	256.5	256.9	379.8	1.405	1.396	1.394	0.943
CH424F100A028	654.5	413.6	416.2	416.6	605.9	1.582	1.573	1.571	1.080
CH588F100A028	1047.2	551.5	555.0	555.4	791.7	1.899	1.887	1.885	1.323
CH243F090A090	453.3	287.0	289.1	291.2	412.1	1.579	1.568	1.557	1.100
CH424F090A090	856.4	443.7	446.7	448.6	636.3	1.930	1.917	1.909	1.346
CH588F090A090	1156.5	579.8	583.6	585.5	820.5	1.995	1.982	1.975	1.410
CH243F090A210	445.2	286.8	288.9	291.0	411.9	1.552	1.541	1.530	1.081
H424F090A210	878.9	443.5	446.5	448.4	636.1	1.982	1.968	1.960	1.382
CH588F090A210	1186.5	579.6	583.4	585.3	820.3	2.047	2.034	2.027	1.446
Mean						1.733	1.720	1.709	1.229
Standard deviation						0.239	0.238	0.241	0.172

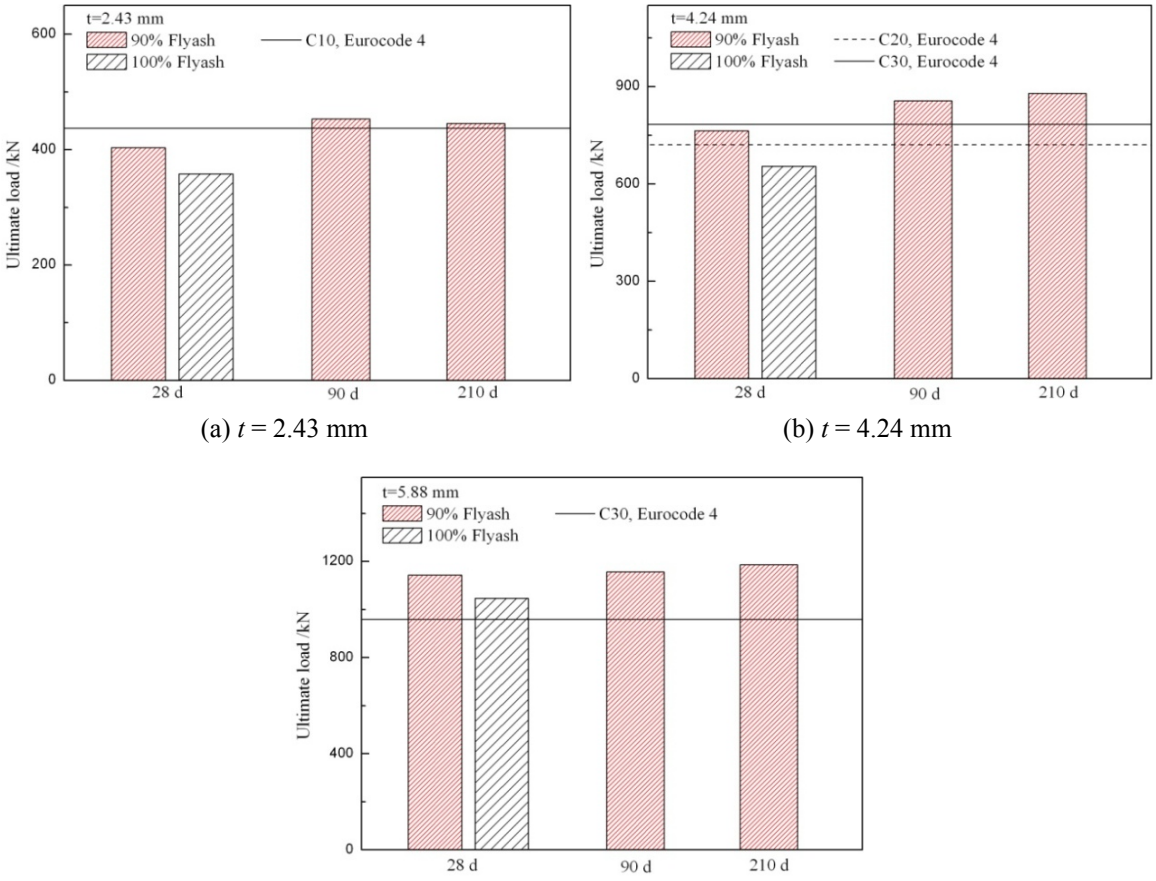

(a) t = 2.43 mm (b) t = 4.24 mm

(c) t = 5.88 mm

Fig. 9 Carrying capacities of CFFST specimens filled with F090 and F100 concrete

4. Conclusions

An experimental study of axially loaded CFFST stub columns is presented in this paper. The influences of flyash content, wall thickness and curing age on the ultimate capacity and the confinement effect of CFFST stub columns are investigated. The experimental results are compared with the ultimate loads predicted using AISC-LRFD, ACI, AIJ and Eurocode 4. The following results of the study are worth noting:

(1) The ultimate capacity of CFFST stub columns is positively correlated with wall thickness and curing age, and negatively correlated with flyash content. The influences of flyash content and curing age on the ultimate capacity are more remarkable for specimens with thin walls. The ultimate capacity of CFFST stub columns depends primarily on the confinement effect of the external steel tube on the concrete core.

(2) The confinement percentage of the CFFST specimens with thick walls increases with flyash content until the latter reaches 90%, and then, it decreases, and it is positively correlated with wall thickness and curing age. The confinement effect occurs earlier in

specimens filled with high-flyash-content concrete than specimens filled with ordinary Portland cement concrete.

(3) Eurocode 4 is more reasonable than AISC-LRFD, ACI and AIJ for predicting the ultimate capacity of CFFST stub columns. Compared with Eurocode 4, a 5.88-mm-thick steel tube filled with 100% flyash concrete is equivalent in strength to a similar steel tube filled with C30 concrete at 28 days, which satisfies the requirements for engineering applications.

Acknowledgments

The financial support from the National Natural Science Foundation of China (51278298, 50978162) is gratefully appreciated.

References

Abdalla, S., Abed, F. and Alhamaydeh, M. (2013), "Behavior of CFSTs and CCFSTs under quasi-static axial compression", *J. Constr. Steel Res.*, **90**, 235-244.

Abed, F., Alhamaydeh, M. and Abdalla, S. (2013), "Experimental and numerical investigations of the compressive behavior of concrete filled steel tubes (CFSTs)", *J. Constr. Steel Res.*, **80**, 429-439.

ACI 318-99 (1999), Building code requirements for structural concrete and commentary, American Concrete Institute, Farmington Hills, Detroit, MI, USA.

AIJ (1997), Recommendations for design and construction of concrete filled steel tubular structures, Architectural Institute of Japan, Tokyo, Japan.

AISC-LRFD (1999), Load and resistance factor design specification for structural steel building, American Institute of Steel Construction, Chicago, IL, USA.

Bilodeau, A. and Malhotra, M. (2000), "High-volume fly ash system: Concrete solution for sustainable development", *ACI Mater. J.*, **97**(1), 41-48.

Chen, B., Liu, X. and Li, S.P. (2011), "Performance investigation of square concrete-filled steel tube columns", *J. Wuhan Univ. Technol.*, **26**(4), 730-736.

Chung, K.S., Kim, J.H. and Yoo, J.H. (2013), "Experimental and analytical investigation of high-strength concrete-filled steel tube square columns subjected to flexural loading", *Steel Compos. Struct., Int. J.*, **14**(2), 133-153.

Dinakar, P. (2012), "Design of self-compacting concrete with fly ash", *Mag. Concr. Res.*, **64**(5), 401-409.

Dinakar, P., Reddy, M.K. and Sharma, M. (2013), "Behaviour of self compacting concrete using Portland pozzolana cement with different levels of fly ash", *Mater. Des.*, **46**, 609-616.

Eurocode 4 (1994), Design of composite steel and concrete structures - Part 1-1: General rules and rules for buildings, British Standards Institution, London, UK.

Evirgen, B., Tuncan, A. and Taskin, K. (2014), "Structural behavior of concrete filled steel tubular sections (CFT/CFSt) under axial compression", *Thin-Wall. Struct.*, **80**, 46-56.

Gupta, P.K., Sarda, S.M. and Kumar, M.S. (2007), "Experimental and computational study of concrete filled steel tubular columns under axial loads", *J. Constr. Steel Res.*, **63**(2), 182-193.

Han, L.H., Yao, G.H. and Zhao, X.L. (2005), "Tests and calculations for hollow structural steel (HSS) stub columns filled with self-consolidating concrete (SCC)", *J. Constr. Steel Res.*, **61**(9), 1214-1269.

Jiang, Z.W., Li, X.T., Sun, Z.P. and Wang, P.M. (2010), "Preparation and application of self-compacting concrete filled with steel pipe arch", *J. Build. Mater.*, **13**(2), 203-209. [In Chinese].

Kayali, O. and Ahmed, M.S. (2013), "Assessment of high volume replacement fly ash concrete - Concept of performance index", *Constr. Build. Mater.*, **39**, 71-76.

Kvedaras, A.K., Sauciuvenas, G., Komka, A. and Jarmolajeva, E. (2015), "Analysis of behaviour for hollow/solid concrete-filled CHS steel beams", *Steel Compos. Struct., Int. J.*, **19**(2), 293-308.

Li, G.Y., Zhao, X.H., Wang, P.M. and Liu, X.P. (2006), "Behaviour of concrete-filled steel tubular columns incorporating flyash", *Cem*. *Concr*. *Compos*., **28**(2), 189-196.
Siddique, R. (2011), "Properties of self-compacting concrete containing class F fly ash", *Mater*. *Des*., **32**(3), 1501-1507.
Xiao, C.Z., Cai, S.H., Chen, T. and Xu, C.L. (2012), "Experimental study on shear capacity of circular concrete filled steel tubes", *Steel Compos*. *Struct*., *Int*. *J*., **13**(5), 437-449.

CC